

Josephson and proximity effects on the surface of a topological insulator

Takehito Yokoyama

Department of Physics, Tokyo Institute of Technology, Tokyo 152-8551, Japan

(Received 14 May 2012; revised manuscript received 21 June 2012; published 3 August 2012)

We investigate Josephson and proximity effects on the surface of a topological insulator on which superconductors and a ferromagnet are deposited. The superconducting regions are described by the conventional BCS Hamiltonian, rather than the superconducting Dirac Hamiltonian. Junction interfaces are assumed to be dirty. We obtain analytical expressions of the Josephson current and the proximity-induced anomalous Green's function on the topological insulator. The dependence of the Josephson effect on the junction length, the temperature, the chemical potential, and the magnetization is discussed. It is also shown that the proximity-induced pairing on the surface of a topological insulator includes even- and odd-frequency triplet pairings as well as a conventional s -wave pairing.

DOI: [10.1103/PhysRevB.86.075410](https://doi.org/10.1103/PhysRevB.86.075410)

PACS number(s): 73.43.Nq, 72.25.Dc, 85.75.-d

I. INTRODUCTION

The topological insulator offers a new state of matter topologically different from the conventional band insulator.¹⁻⁶ Edge channels or surface states of the topological insulator are topologically protected and described by Dirac fermions at low energies. The nature of the surface Dirac fermion of the topological insulator manifests itself in interesting phenomena, such as the quantized magnetoelectric effect,^{7,8} giant spin rotation,⁹ magnetic properties of the surface state,¹⁰ magnetization dynamics,¹¹⁻¹³ magnetotransport phenomena,¹⁴⁻¹⁹ and the superconducting proximity effect.²⁰⁻²⁴

There has been a great and increasing interest in topological insulators attached to superconductors. In particular, Majorana fermions emerging in these systems have been investigated intensively.^{25,26} When superconductor/ferromagnet junctions are deposited on topological insulators, surface Dirac fermions acquire a domain wall structure of the mass. At the domain wall, Majorana fermions emerge as a zero energy bound state.^{27,28} Majorana fermions have received much interest from the viewpoint of fundamental physics and also fault-tolerant quantum computing due to their exotic properties.^{25,26} It has also been shown that Majorana bound states crucially influence the Josephson effect. The current-phase relation shows 4π periodicity, i.e., $\sin(\phi/2)$ with the phase difference across the junction ϕ .²⁸⁻³⁰ In previous works,^{23-26,28} it was assumed that the Dirac fermions become superconducting due to the proximity effect, and the junctions between superconducting and normal Dirac fermions were considered. In this paper, we take a different modeling of the same system. We consider the coupling between conventional superconductors and a topological insulator, rather than that between superconducting and normal (or magnetic) Dirac fermions.³¹⁻³³ Namely, tunneling between the Schrödinger electrons and the Dirac fermions is explicitly taken into account. Here, the superconductors are topologically trivial, and hence, in this setup, no Majorana fermions appear.

In this paper, we study Josephson and proximity effects on the surface of a topological insulator on which superconductors and a ferromagnet are deposited. The superconducting regions are described by the conventional BCS Hamiltonian rather than superconducting Dirac electrons. We consider disordered junction interfaces in contrast to the previous works.^{23-26,28}

We obtain analytical expressions of the Josephson current and the proximity-induced anomalous Green's function on the topological insulator. The dependence of the Josephson effect on the junction length, the temperature, the chemical potential, and the magnetization is discussed. It is also shown that the proximity-induced pairing on the surface of a topological insulator includes even- and odd-frequency triplet pairings^{34,35} as well as a conventional s -wave pairing.

Previous works on the Josephson effect on the surface of a topological insulator are mostly based on the approach that takes into account only the contribution from the Andreev bound states.^{23,24,28} This holds for short junctions with $d \ll \xi$, where d and ξ are the junction length and the superconducting coherence length, respectively.³⁶ In this paper, we adopt the functional integral method,^{37,38} which is applicable to any length of the junction,^{39,40} thus allowing us to study the asymptotic behavior of the Josephson current for $d \rightarrow \infty$.

II. FORMULATION

We consider superconductor/topological insulator/superconductor junctions where a ferromagnet is also attached to the topological insulator, as shown in Fig. 1(a). Junctions without the ferromagnetic region [Fig. 1(b)] can be considered just by setting the exchange field to zero in the ferromagnetic region. The total Hamiltonian of the system reads

$$H = H_L + H_R + H_M + H_T, \quad (1)$$

where^{20,40}

$$H_{L(R)} = \sum_{\mathbf{k}_{L(R)}} \phi_{\mathbf{k}_{L(R)}}^\dagger \xi_{\mathbf{k}_{L(R)}} \sigma_0 \otimes \tau_3 \phi_{\mathbf{k}_{L(R)}} + \sum_{\mathbf{k}_{L(R)}} \phi_{\mathbf{k}_{L(R)}}^\dagger [\Delta e^{-i\varphi_{L(R)}\tau_3} \sigma_0 \otimes \tau_1] \phi_{\mathbf{k}_{L(R)}}, \quad (2)$$

$$H_M = \sum_{\mathbf{k}} \phi_{\mathbf{k}}^\dagger [\hbar v_F (k_y \sigma^x - k_x \sigma^y) \otimes \tau_3 + \mathbf{m} \cdot \boldsymbol{\sigma} \otimes \tau_0 - \mu \sigma_0 \otimes \tau_3] \phi_{\mathbf{k}}, \quad (3)$$

$$H_T = \sum_{\mathbf{k}, \mathbf{k}_L} \phi_{\mathbf{k}_L}^\dagger [t e^{i(\mathbf{k}-\mathbf{k}_L) \cdot \mathbf{r}_L} \sigma_0 \otimes \tau_3] \phi_{\mathbf{k}} + \sum_{\mathbf{k}, \mathbf{k}_R} \phi_{\mathbf{k}_R}^\dagger [t e^{i(\mathbf{k}-\mathbf{k}_R) \cdot \mathbf{r}_R} \sigma_0 \otimes \tau_3] \phi_{\mathbf{k}} + \text{H.c.}, \quad (4)$$

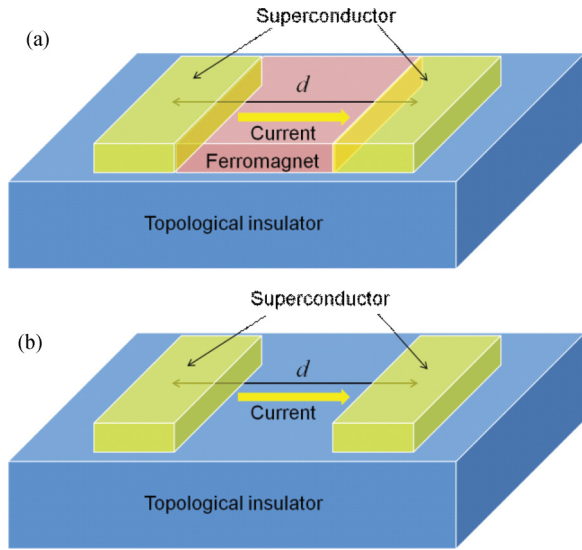


FIG. 1. (Color online) Schematic of the model.

with $\xi_{\mathbf{k}L(R)} = \frac{\hbar^2 \mathbf{k}^2}{2m} - \mu_{L(R)}$ and $\phi_{\mathbf{k}L(R)}^\dagger = (c_{\mathbf{k}L(R)\uparrow}^\dagger, c_{\mathbf{k}L(R)\downarrow}^\dagger, ic_{-\mathbf{k}L(R)\downarrow}, -ic_{-\mathbf{k}L(R)\uparrow})$. Here, Δ and $\varphi_{L(R)}$ are the magnitude of the gap function and the phase of the left (right) superconductor, respectively. Also, \mathbf{m} is the exchange field, and σ and τ are Pauli matrices in spin and Nambu spaces, respectively. $H_{L(R)}$ represents the Hamiltonian on the left (right) superconductor, while H_M is the Dirac Hamiltonian with the exchange field. Note that the superconductors are described by the Schrödinger electrons and are topologically trivial. Hence, in this setup, no Majorana fermions emerge.⁴¹ H_T is the tunneling Hamiltonian between the superconductors and the surface of the topological insulator, which is treated as a perturbation. $\mathbf{r}_{L(R)}$ is the position of the interface between the left (right) superconductor and the topological insulator. We consider the incoherent tunneling model where the spin is conserved but the momentum is not conserved upon tunneling at the interface. This modeling is applicable to junctions with imperfect dirty insulating barriers.⁴² In real space representation, the tunneling matrix element reads $t\delta(\mathbf{r} - \mathbf{r}_{L(R)})$. The average of the position vectors is assumed to give $\langle |\mathbf{r}_R - \mathbf{r}_L| \rangle = d$.⁴⁰ The calculated results are averaged over the positions of \mathbf{r}_L and \mathbf{r}_R at the interfaces.

The partition function is then given by

$$Z = \int D\bar{\psi} D\psi \exp \left[- \sum_{\{\mathbf{k}\}} \bar{\psi} (-G_0^{-1} + \hat{T}) \psi \right], \quad (5)$$

where $\bar{\psi} = (\bar{\phi}_{\mathbf{k}L}, \bar{\phi}_{\mathbf{k}}, \bar{\phi}_{\mathbf{k}R})$. G_0 is the bulk Green's function while \hat{T} is a tunneling matrix. See the Appendix for their explicit forms. The free energy of the system can be calculated as $F = -T \ln Z$, where T is the temperature of the system. The leading contribution to the Josephson current is given by the fourth order with respect to the tunneling Hamiltonian (see the Appendix for the details of the calculation). The Josephson current is then calculated as

$$I = -\frac{2e}{\hbar} \frac{\partial F}{\partial \varphi} = -\frac{4e}{\hbar} T t^4 \sin(\varphi + 2m_y d / \hbar v_F) \sum_{\omega_n} \frac{(vV\Delta)^2}{\omega_n^2 + \Delta^2} \times [|\hbar v_F k_F|^2 |K_1(k_F d)|^2 - (\omega_n^2 + \mu^2 - m_z^2) |K_0(k_F d)|^2], \quad (6)$$

where v , V , ω_n , and $K_\nu(z)$ ($\nu = 0, 1$) are, respectively, the density of states at the Fermi level, the area of the surface of the topological insulator sandwiched between the superconductors, the fermionic Matsubara frequency, and the modified Bessel function. Also, k_F is defined by $\hbar v_F k_F = \sqrt{(\omega_n - i\mu)^2 + m_z^2}$ and the branch is taken so that $\text{Re} k_F > 0$. Here, $\varphi = \varphi_R - \varphi_L$ is the phase difference across the junction. It is seen that the Josephson effect is independent of m_x , and m_y shifts the phase difference.^{23,24}

The critical current I_C can be written as

$$\frac{-eI_C R}{T_C} = \frac{T}{T_C} \left(\frac{d}{\hbar v_F} \right)^2 \sum_{\omega_n} \frac{\Delta^2}{\omega_n^2 + \Delta^2} [|\hbar v_F k_F|^2 |K_1(k_F d)|^2 - (\omega_n^2 + \mu^2 - m_z^2) |K_0(k_F d)|^2], \quad (7)$$

where T_C is the superconducting transition temperature and

$$R^{-1} = \frac{4e^2}{\hbar} \left(\frac{t^2 V v}{d} \right)^2. \quad (8)$$

III. RESULTS

A. Josephson effect

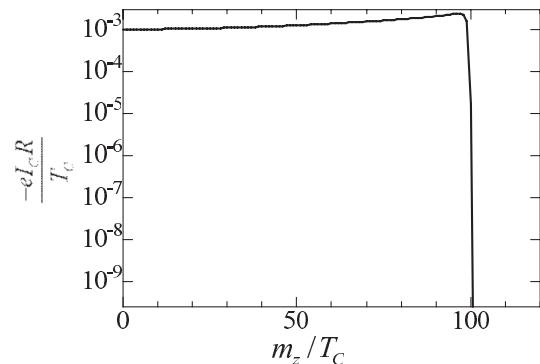
In what follows, we will study the critical Josephson current using Eq. (7). We consider a temperature dependence of the gap of the BCS type modeled by⁴³

$$\Delta(T) = \Delta(0) \tanh(1.74 \sqrt{T_C/T - 1}). \quad (9)$$

1. The effect of the exchange field

Here, let us study the effect of the exchange field. As seen from Eq. (7), the Josephson effect is independent of m_x , and m_y shifts the phase difference. Since the in-plane exchange field corresponds to the shift of the momentum,¹⁴ the effect of the in-plane exchange field can be reduced to the phase factor [which can be seen by proper transformations in Eq. (A8)], and hence we find the phase shift proportional to m_y .

To see the effect of the z component of the exchange field, m_z , we plot the dependence of the critical Josephson current on m_z in Fig. 2 for $T/T_C = 0.1$, $d/\xi = 1$, and $\mu/T_C = 100$, where $\xi = \hbar v_F / T_C$ is the superconducting coherence length. With increasing m_z , I_C increases, and for $m_z > \mu$, the current is strongly suppressed. This is because for $m_z > \mu$, the Fermi level lies inside the mass gap and hence the surface state of the


 FIG. 2. Critical Josephson current as a function of m_z for $T/T_C = 0.1$, $d/\xi = 1$, and $\mu/T_C = 100$.

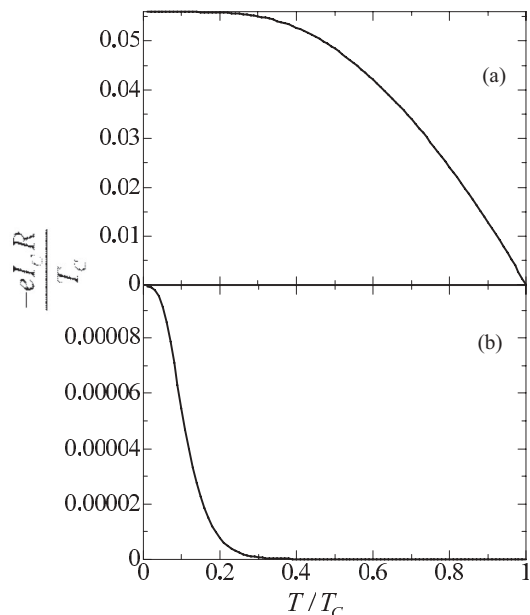


FIG. 3. Critical Josephson current as a function of temperature of the system with $m_z = 0$ and $\mu/T_C = 100$ for (a) $d/\xi = 0.1$ and (b) $d/\xi = 5$.

topological insulator is no longer metallic. Note that the surface spectrum is given by $E_M = \pm\sqrt{k^2 + m_z^2} \pm \mu$ (here we set $m_x = m_y = 0$ for simplicity). Also, it should be noted that since the superconductors are topologically trivial, there is no edge state or Majorana bound state. This is in stark contrast to similar junctions where superconducting regions are described by Dirac fermions: there, the Majorana bound state can carry the Josephson current.^{23,24,28}

2. Superconductor/topological insulator/superconductor junction

Now, we will investigate the Josephson junction characteristics. Since the effects of the exchange field have been clarified, here let us consider the junction with $\mathbf{m} = \mathbf{0}$. This corresponds to the junction illustrated in Fig. 1(b).

Figure 3 depicts the T dependence of the critical Josephson current with $\mu/T_C = 100$ for (a) $d/\xi = 0.1$ and (b) $d/\xi = 5$. For short normal segment $d/\xi = 0.1$, the behavior is similar to that of the conventional Josephson junctions through an insulating barrier, i.e., $\tanh(\Delta/2T)$.⁴⁴ For large d , the critical current shows an exponential decay. This can also be obtained as follows. Using the asymptotic form of the modified Bessel function for $|z| \gg 1$:

$$K_\nu(z) \sim \sqrt{\frac{\pi}{2z}} e^{-z} \left[1 + \frac{(4\nu^2 - 1)}{8z} + \dots \right] \quad (10)$$

for $m_z = 0$, $Td/\hbar v_F \gg 1$, and $\mu \gg T$, we have

$$\frac{-eI_C R}{T_C} \sim \frac{1}{2\mu T_C} \frac{(\pi T \Delta)^2}{(\pi T)^2 + \Delta^2} e^{-2\pi T d/\hbar v_F}. \quad (11)$$

Notice that the $n = 0$ component in the Matsubara frequencies has a dominant contribution to the Josephson current. This form shows a typical exponential decay of the critical Josephson current for $Td/\hbar v_F \gg 1$: the asymptotic behavior of the Josephson current (the exponential decay) has the same form as that governed by the Schrödinger electrons.^{40,45}

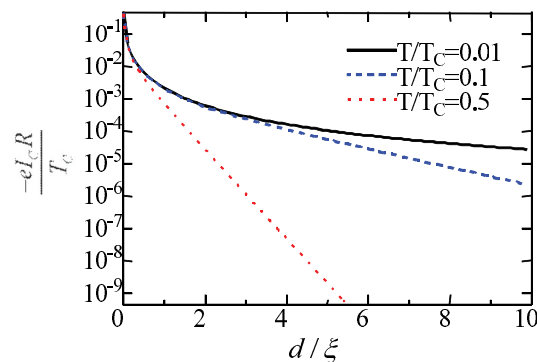


FIG. 4. (Color online) Critical Josephson current as a function of the distance between the superconductors d for $m_z = 0$, $\mu/T_C = 100$, and several temperatures.

In Fig. 4, we show the d dependence of the critical Josephson current for $\mu/T_C = 100$ and several temperatures. For large d or at high temperature, we see an exponential decay of the critical Josephson current. This is also consistent with the above analytical expression.

Figure 5 shows the μ dependence of the critical Josephson current for $T/T_C = 0.1$ and several d . It is found that with the increase of μ , the critical current decreases monotonically. This is because the proximity effect is suppressed by increasing the chemical potential μ , as will be shown in Eq. (17). For large d , the Josephson current is inversely proportional to the chemical potential, as seen from Eq. (11). Experimentally, the chemical potential can be tuned by chemical doping⁴⁷ or gating.⁴⁸

Recently, Josephson supercurrent through a topological insulator surface state has been observed.⁴⁶ The dependence on T and d shown in Figs. 3 and 4 is qualitatively consistent with the experimental data. A quantitative difference would come from the fact that the bulk states of the topological insulator also contribute to the Josephson current because the chemical potential of the sample used in Ref. 46 probably crosses the bulk bands.

B. Proximity effect

In this subsection, we will investigate the proximity effect in a topological insulator/ s -wave superconductor junction. The proximity effect in this junction has been investigated in Refs. 31–33. The tunneling between the superconductor

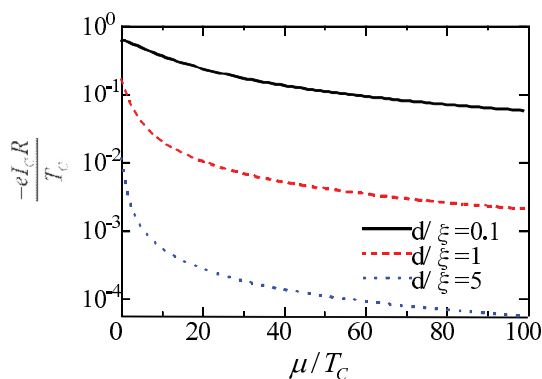


FIG. 5. (Color online) Critical Josephson current as a function of the chemical potential μ for $m_z = 0$, $T/T_C = 0.1$, and several d .

and a bulk topological insulator has been considered, and the validity of the Fu-Kane model has been discussed, based on mostly numerical approaches.^{31–33}

Here, we consider the tunneling between the superconductor and the *surface* of the topological insulator. Using the functional integral method, we derive analytical expressions of the proximity-induced anomalous Green's functions on the topological insulator.

Now, let us consider superconductor/topological insulator bilayer junctions. To do so, let us remove the degree of freedom of the right superconductor from the above formulation (see also the Appendix). Without loss of generality, we can set $\varphi_L = 0$ and $\mathbf{r}_L = \mathbf{0}$. The Green functions can be calculated as

$$G = \int D\bar{\psi} D\psi \psi \bar{\psi} \exp \left[- \sum_{\langle \mathbf{k} \rangle} \bar{\psi} (-G_0^{-1} + \hat{T}) \psi \right], \quad (12)$$

where $\bar{\psi} = (\bar{\phi}_{\mathbf{k}_L}, \bar{\phi}_{\mathbf{k}})$. Performing the functional integral, we have

$$G = (G_0^{-1} - \hat{T})^{-1} = G_0 \sum_n (\hat{T} G_0)^n, \quad (13)$$

where

$$G = \begin{pmatrix} G'_L & 0 \\ 0 & G'_M \end{pmatrix}, \quad G_0 = \begin{pmatrix} G_L & 0 \\ 0 & G_M \end{pmatrix},$$

$$\hat{T} = \begin{pmatrix} 0 & T_{12} \\ T_{21} & 0 \end{pmatrix}. \quad (14)$$

The leading contribution is given by the second order with respect to the tunneling matrix. The anomalous Green's function on the surface of the topological insulator f'_M in the second order in t can be represented as

$$f'_M = -t^2 g_M(\mathbf{k}, \omega_n) \bar{g}_M(\mathbf{k}, \omega_n) \sum_{\mathbf{k}_L} f_L(\mathbf{k}_L, \omega_n) \quad (15)$$

$$= \frac{\pi v \Delta t^2}{\sqrt{\omega_n^2 + \Delta^2}} \frac{-[\omega_n^2 + \mu^2 + (\hbar v_F k)^2] + m^2 - 2\mu \hbar v_F \mathbf{k}_\perp \cdot \boldsymbol{\sigma} + 2i\omega_n \mathbf{m} \cdot \boldsymbol{\sigma} + 2i\hbar v_F (\mathbf{k}_\perp \times \mathbf{m}) \cdot \boldsymbol{\sigma}}{[i(\omega_n + \mu)^2 - (\hbar v_F)^2 \{(k_y + m_x)^2 + (k_x - m_y)^2\} - m_z^2][i(\omega_n - \mu)^2 - (\hbar v_F)^2 \{(k_y - m_x)^2 + (k_x + m_y)^2\} - m_z^2]} \quad (16)$$

with $\mathbf{k}_\perp = (k_y, -k_x, 0)$. Here, spin-singlet pairing is proportional to the unit matrix in spin space while spin-triplet pairing is proportional to the Pauli matrix $\boldsymbol{\sigma}$. Therefore, it is seen that both singlet and triplet pairings are induced on the surface of the topological insulator. The generation of the triplet pairing reflects the symmetry breaking in spin space.⁴⁹ In particular, for $\mathbf{m} = \mathbf{0}$, we have

$$f'_M = \frac{\pi v \Delta t^2}{\sqrt{\omega_n^2 + \Delta^2}} \times \frac{-[\omega_n^2 + \mu^2 + (\hbar v_F k)^2] - 2\mu \hbar v_F \mathbf{k}_\perp \cdot \boldsymbol{\sigma}}{(\omega_n^2 + \mu^2)^2 + (\hbar v_F k)^4 + 2(\hbar v_F k)^2 (\omega_n^2 - \mu^2)}. \quad (17)$$

We see that in the limit of $\mu \rightarrow \infty$, we have $f'_M \rightarrow 0$. This explains the suppression of the Josephson current with μ in Fig. 5. It is also found that even in the absence of the exchange

$$F(k_x, k_y, \omega_n) = \frac{\pi v \Delta t^2}{\sqrt{\omega_n^2 + \Delta^2}} \frac{1}{[\omega_n^2 + (\hbar v_F)^2 \{(k_y + m_x)^2 + (k_x - m_y)^2\} + m_z^2][\omega_n^2 + (\hbar v_F)^2 \{(k_y - m_x)^2 + (k_x + m_y)^2\} + m_z^2]}. \quad (19)$$

Note that $F(k_x, k_y, \omega_n)$ is an even function of $\mathbf{k} [= (k_x, k_y, 0)]$ and ω_n . We find that the component proportional to $-\omega_n^2 - (\hbar v_F k)^2 + m^2$ represents a singlet s -wave superconductivity, while that proportional to

field, triplet pairing is induced on the surface if $\mu \neq 0$, which is consistent with Refs. 31 and 32 (see also Ref. 50). In previous works, it was assumed that by attaching an s -wave superconductor to a topological insulator, the same s -wave superconductivity is induced on the surface.^{23–26,28} Here, we find that not only s -wave singlet superconductivity but, in general, triplet p -wave superconductivity is also induced on the surface of the topological insulator.^{31,32} Also, we assume here clean surface states on the topological insulator. If the surface is in the diffusive regime, it is expected that odd-frequency triplet s -wave superconductivity is induced on the topological insulator.⁵¹

Let us focus on the case with $\mu = 0$ but finite exchange field. The anomalous Green's function then becomes

$$f'_M = F(k_x, k_y, \omega_n) [-\omega_n^2 - (\hbar v_F k)^2 + m^2 + 2i\omega_n \mathbf{m} \cdot \boldsymbol{\sigma} + 2i\hbar v_F (\mathbf{k}_\perp \times \mathbf{m}) \cdot \boldsymbol{\sigma}], \quad (18)$$

$2i\omega_n \mathbf{m} \cdot \boldsymbol{\sigma}$ is triplet and odd in ω_n , namely odd-frequency triplet s -wave pairing.^{34,35} The component proportional to $2i(\mathbf{k}_\perp \times \mathbf{m}) \cdot \boldsymbol{\sigma}$ corresponds to a triplet p -wave superconductivity.

IV. SUMMARY

In this paper, we have investigated Josephson and proximity effects on the surface of a topological insulator on which superconductors and a ferromagnet are deposited. We have described the superconducting regions by the conventional BCS Hamiltonian rather than the superconducting Dirac Hamiltonian. We have presented analytical expressions of the Josephson current and the proximity-induced anomalous Green's function on the topological insulator. The dependence of the Josephson effect on the junction length, the temperature, the chemical potential, and the magnetization has been discussed. It has also been shown that the proximity-induced pairing on the surface of a topological insulator includes even- and odd-frequency triplet pairings as well as a conventional s -wave pairing.

ACKNOWLEDGMENTS

This work was supported by a Grant-in-Aid for Young Scientists (B) (No. 23740236) and the "Topological Quantum Phenomena" (No. 23103505) Grant-in-Aid for Scientific

Research on Innovative Areas from the Ministry of Education, Culture, Sports, Science and Technology (MEXT) of Japan.

APPENDIX: CALCULATION OF THE FREE ENERGY

In this appendix, we present the details of the calculation of the free energy of the junctions. The unperturbed Green's function G_0 is represented by a 12×12 matrix as

$$G_0^{-1} = \begin{pmatrix} G_L^{-1} & 0 & 0 \\ 0 & G_M^{-1} & 0 \\ 0 & 0 & G_R^{-1} \end{pmatrix}, \quad (\text{A1})$$

$$G_{L(R)} = -\frac{i\omega_n \sigma_0 \otimes \tau_0 + \xi_{\mathbf{k}_{L(R)}} \sigma_0 \otimes \tau_3 + \Delta e^{-i\varphi_{L(R)}\tau_3} \sigma_0 \otimes \tau_1}{\omega_n^2 + \xi_{\mathbf{k}_{L(R)}}^2 + \Delta^2} \\ \equiv \begin{pmatrix} g_{L(R)} & f_{L(R)} \\ \bar{f}_{L(R)} & \bar{g}_{L(R)} \end{pmatrix}, \quad (\text{A2})$$

$$G_M = \begin{pmatrix} \frac{i\omega_n + \mu + \hbar v_F(k_y + m_x)\sigma^x - \hbar v_F(k_x - m_y)\sigma^y + m_z\sigma^z}{(i\omega_n + \mu)^2 - (\hbar v_F)^2\{(k_y + m_x)^2 + (k_x - m_y)^2\} - m_z^2} & 0 \\ 0 & \frac{i\omega_n - \mu - \hbar v_F(k_y - m_x)\sigma^x + \hbar v_F(k_x + m_y)\sigma^y + m_z\sigma^z}{(i\omega_n - \mu)^2 - (\hbar v_F)^2\{(k_y - m_x)^2 + (k_x + m_y)^2\} - m_z^2} \end{pmatrix} \equiv \begin{pmatrix} g_M & 0 \\ 0 & \bar{g}_M \end{pmatrix}. \quad (\text{A3})$$

By performing the functional integral, we have the free energy of the junctions of the form

$$F = -T \ln Z = -T \text{Tr} \ln [-G_0^{-1} + \hat{T}], \quad (\text{A4})$$

where \hat{T} is the tunneling matrix given by

$$\hat{T} = \begin{pmatrix} 0 & T_{12} & 0 \\ T_{21} & 0 & T_{23} \\ 0 & T_{32} & 0 \end{pmatrix} \quad (\text{A5})$$

with $T_{12} = t e^{i(\mathbf{k}-\mathbf{k}_L)\cdot\mathbf{r}_L} \sigma_0 \otimes \tau_3 = T_{21}^*$ and $T_{23} = t e^{i(\mathbf{k}_R-\mathbf{k})\cdot\mathbf{r}_R} \sigma_0 \otimes \tau_3 = T_{32}^*$.

The leading contribution is given by the fourth order with respect to the tunneling element, which is calculated as

$$F \approx -\frac{T}{4} \text{Tr}(G_0 \hat{T})^4 \quad (\text{A6})$$

$$= -T \text{Tr} \sum_{\mathbf{k}_L, \mathbf{k}, \mathbf{k}_R, \mathbf{k}', \omega_n} G_L(\mathbf{k}_L, \omega_n) T_{12} G_M(\mathbf{k}, \omega_n) T_{23} G_R(\mathbf{k}_R, \omega_n) T_{32} G_M(\mathbf{k}', \omega_n) T_{21} \quad (\text{A7})$$

$$= 2T t^4 \text{Tr} \text{Re} \left[\sum_{\mathbf{k}_L, \mathbf{k}, \mathbf{k}_R, \mathbf{k}', \omega_n} e^{i(\mathbf{k}-\mathbf{k}')\cdot(\mathbf{r}_R-\mathbf{r}_L)} f_L(\mathbf{k}_L, \omega_n) \bar{g}_M(\mathbf{k}, \omega_n) \bar{f}_R(\mathbf{k}_R, \omega_n) g_M(\mathbf{k}', \omega_n) \right] \quad (\text{A8})$$

$$= -2T t^4 \cos(\varphi + 2m_y d / \hbar v_F) \sum_{\omega_n} \frac{(vV\Delta)^2}{\omega_n^2 + \Delta^2} [|\hbar v_F k_F|^2 |K_1(k_F d)|^2 - (\omega_n^2 + \mu^2 - m_z^2) |K_0(k_F d)|^2]. \quad (\text{A9})$$

Here, we have used the following relations:

$$J_0(x) = \frac{1}{2\pi} \int_0^{2\pi} e^{ix \cos \varphi} d\varphi, \quad K_0(ak) = \int_0^\infty \frac{x J_0(ax)}{x^2 + k^2} dx, \quad K_1(x) = -\frac{d}{dx} K_0(x) \quad (\text{A10})$$

for $a > 0$ and $\text{Re} k > 0$, where $J_0(x)$ is the Bessel function.

- ¹J. E. Moore and L. Balents, *Phys. Rev. B* **75**, 121306(R) (2007).
- ²L. Fu, C. L. Kane, and E. J. Mele, *Phys. Rev. Lett.* **98**, 106803 (2007).
- ³A. P. Schnyder, S. Ryu, A. Furusaki, and A. W. W. Ludwig, *Phys. Rev. B* **78**, 195125 (2008).
- ⁴X.-L. Qi and S.-C. Zhang, *Phys. Today* **63**(1), 33 (2010).
- ⁵M. Z. Hasan and C. L. Kane, *Rev. Mod. Phys.* **82**, 3045 (2010).
- ⁶X.-L. Qi and S.-C. Zhang, *Rev. Mod. Phys.* **83**, 1057 (2011).
- ⁷X.-L. Qi, T. Hughes, and S.-C. Zhang, *Nat. Phys.* **4**, 273 (2008).
- ⁸X.-L. Qi, T. L. Hughes, and S.-C. Zhang, *Phys. Rev. B* **78**, 195424 (2008).
- ⁹T. Yokoyama, Y. Tanaka, and N. Nagaosa, *Phys. Rev. Lett.* **102**, 166801 (2009).
- ¹⁰Q. Liu, C.-X. Liu, C. Xu, X.-L. Qi, and S.-C. Zhang, *Phys. Rev. Lett.* **102**, 156603 (2009).
- ¹¹I. Garate and M. Franz, *Phys. Rev. Lett.* **104**, 146802 (2010).
- ¹²T. Yokoyama, J. Zang, and N. Nagaosa, *Phys. Rev. B* **81**, 241410(R) (2010).
- ¹³T. Yokoyama, *Phys. Rev. B* **84**, 113407 (2011).
- ¹⁴T. Yokoyama, Y. Tanaka, and N. Nagaosa, *Phys. Rev. B* **81**, 121401(R) (2010).
- ¹⁵I. Garate and M. Franz, *Phys. Rev. B* **81**, 172408 (2010).
- ¹⁶S. Mondal, D. Sen, K. Sengupta, and R. Shankar, *Phys. Rev. Lett.* **104**, 046403 (2010).
- ¹⁷A. A. Burkov and D. G. Hawthorn, *Phys. Rev. Lett.* **105**, 066802 (2010).
- ¹⁸T. Yokoyama and S. Murakami, *Phys. Rev. B* **83**, 161407(R) (2011).
- ¹⁹D. Culcer, *Physica E* **44**, 860 (2012).
- ²⁰L. Fu and C. L. Kane, *Phys. Rev. Lett.* **100**, 096407 (2008).
- ²¹L. Fu and C. L. Kane, *Phys. Rev. Lett.* **102**, 216403 (2009).
- ²²A. R. Akhmerov, J. Nilsson, and C. W. J. Beenakker, *Phys. Rev. Lett.* **102**, 216404 (2009).
- ²³Y. Tanaka, T. Yokoyama, and N. Nagaosa, *Phys. Rev. Lett.* **103**, 107002 (2009).
- ²⁴J. Linder, Y. Tanaka, T. Yokoyama, A. Sudbø, and N. Nagaosa, *Phys. Rev. Lett.* **104**, 067001 (2010); *Phys. Rev. B* **81**, 184525 (2010).
- ²⁵C. W. J. Beenakker, arXiv:1112.1950v2.
- ²⁶J. Alicea, *Rep. Prog. Phys.* **75**, 076501 (2012).
- ²⁷W. P. Su, J. R. Schrieffer, and A. J. Heeger, *Phys. Rev. B* **22**, 2099 (1980).
- ²⁸L. Fu and C. L. Kane, *Phys. Rev. B* **79**, 161408(R) (2009).
- ²⁹A. Y. Kitaev, *Phys. Usp.* **44**, 131 (2001).
- ³⁰H. J. Kwon, K. Sengupta, and V. M. Yakovenko, *Eur. Phys. J. B* **37**, 349 (2003).
- ³¹T. D. Stanescu, J. D. Sau, R. M. Lutchyn, and S. Das Sarma, *Phys. Rev. B* **81**, 241310(R) (2010).
- ³²M. Lababidi and E. Zhao, *Phys. Rev. B* **83**, 184511 (2011).
- ³³R. Grein, J. Michelsen, and M. Eschrig, arXiv:1111.0445v1.
- ³⁴V. L. Berezinskii, *JETP Lett.* **20**, 287 (1974).
- ³⁵Y. Tanaka, M. Sato, and N. Nagaosa, *J. Phys. Soc. Jpn.* **81**, 011013 (2012).
- ³⁶C. W. J. Beenakker, *Phys. Rev. Lett.* **67**, 3836 (1991).
- ³⁷V. N. Popov, *Functional Integrals and Collective Excitations* (Cambridge University Press, Cambridge, 1987).
- ³⁸N. Nagaosa, *Quantum Field Theory in Condensed Matter Physics* (Springer, Berlin, 1999).
- ³⁹K. Awaka and H. Fukuyama, *J. Phys. Soc. Jpn.* **66**, 2820 (1997).
- ⁴⁰M. Mori, S. Hikino, S. Takahashi, and S. Maekawa, *J. Phys. Soc. Jpn.* **76**, 054705 (2007).
- ⁴¹In Ref. 20, it is assumed that a finite gap function is induced on the surface of a topological insulator by the proximity effect. On the other hand, in this paper, we assume that the surface state of a topological insulator does not acquire a finite gap function, although a superconducting correlation is induced.
- ⁴²For a clean and flat interface, the momentum parallel to the interface should be conserved due to translation invariance along the interface.
- ⁴³B. Muhlshlegel, *Z. Phys.* **155**, 313 (1959).
- ⁴⁴V. Ambegaokar and A. Baratoff, *Phys. Rev. Lett.* **10**, 486 (1963).
- ⁴⁵A. A. Golubov, M. Yu. Kupriyanov, and E. Il'ichev, *Rev. Mod. Phys.* **76**, 411 (2004).
- ⁴⁶M. Veldhorst, M. Snelder, M. Hoek, T. Gang, V. K. Guduru, X. L. Wang, U. Zeitler, W. G. van der Wiel, A. A. Golubov, H. Hilgenkamp, and A. Brinkman, *Nat. Mater.* **11**, 417 (2012).
- ⁴⁷D. Hsieh, Y. Xia, D. Qian, L. Wray, J. H. Dil, F. Meier, J. Osterwalder, L. Patthey, J. G. Checkelsky, N. P. Ong, A. V. Fedorov, H. Lin, A. Bansil, D. Grauer, Y. S. Hor, R. J. Cava, and M. Z. Hasan, *Nature (London)* **460**, 1101 (2009).
- ⁴⁸J. Chen, H. J. Qin, F. Yang, J. Liu, T. Guan, F. M. Qu, G. H. Zhang, J. R. Shi, X. C. Xie, C. L. Yang, K. H. Wu, Y. Q. Li, and L. Lu, *Phys. Rev. Lett.* **105**, 176602 (2010).
- ⁴⁹F. S. Bergeret, A. F. Volkov, and K. B. Efetov, *Phys. Rev. Lett.* **86**, 4096 (2001); *Rev. Mod. Phys.* **77**, 1321 (2005).
- ⁵⁰L. P. Gor'kov and E. I. Rashba, *Phys. Rev. Lett.* **87**, 037004 (2001).
- ⁵¹Y. Asano and Y. Tanaka, arXiv:1204.4226v1.